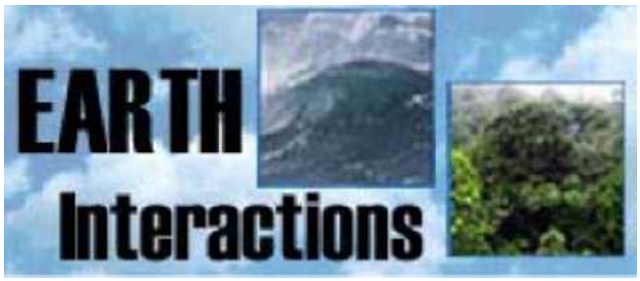

Synthetic Aperture Radar (L band) and Optical Vegetation Indices for Discriminating the Brazilian Savanna Physiognomies: A Comparative Analysis

Edson E. Sano*

Brazilian Agricultural Research Organization, Planaltina, DF, Brazil

Laerte G. Ferreira

Federal University of Goiás, Goiânia, GO, Brazil

Alfredo R. Huete

The University of Arizona, Tucson, Arizona

Received 11 July 2004; accepted 4 May 2005

ABSTRACT: The all-weather capability, signal independence to the solar illumination angle, and response to 3D vegetation structures are the highlights of active radar systems for natural vegetation mapping and monitoring. However, they may present significant soil background effects. This study addresses a comparative analysis of the performance of L-band synthetic aperture radar (SAR) data and optical vegetation indices (VIs) for discriminating the Brazilian cerrado physiognomies. The study area was the Brasilia National Park, Brazil,

* Corresponding author address: Edson E. Sano, Brazilian Agricultural Research Organization—Embrapa, BR-020 km 18 Cx. Postal 08223, CEP: 73301-970 Planaltina DF, Brazil.
E-mail address: sano@cpac.embrapa.br

one of the test sites of the Large-Scale Biosphere–Atmosphere (LBA) experiment in Amazonia. Seasonal *Japanese Earth Resources Satellite-1* (*JERS-1*) SAR backscatter coefficients (σ°) were compared with two vegetation indices [normalized difference vegetation index (NDVI) and enhanced vegetation index (EVI)] over the five most dominant cerrados' physiognomies plus gallery forest. In contrast to the VIs, σ° from dry and wet seasons did not change significantly, indicating primary response to vegetation structures. Discriminant analysis and analysis of variance (ANOVA) showed an overall higher performance of radar data. However, when both SAR and VIs are combined, the discrimination capability increased significantly, indicating that the fusion of the optical and radar backscatter observations provides overall improved classifications of the cerrado types. In addition, VIs showed good performance for monitoring the cerrado dynamics.

KEYWORDS: Cerrado monitoring; SAR; Vegetation index

1. Introduction

Understanding land-cover conversion and dynamics is one of the key research topics of the Large-Scale Biosphere–Atmosphere (LBA) experiment in Amazonia because changes in the land surface affect water, energy, nutrient, and carbon cycle in this region and its surrounding ecosystems (Roberts et al. 2003). The dominant biome in the southern border of the Amazonia is the semideciduous tropical savanna, locally known as the "cerrado." Cerrado is an upland, species-rich ecosystem with more than 450 vascular species per hectare, and occurs mostly in low-fertility and high-aluminum-toxicity oxisols (Eiten 1993). In terms of climate, it presents two well-defined seasons: six months of dry conditions, from May to October, and six months of wet conditions, from November to April. The gentle topography, relatively low land prices, and the construction of Brasilia in 1964 have contributed greatly to convert natural vegetation into cultivated pastures and annual crops (mainly soybean and corn). Nowadays, cerrado is the main agricultural province in Brazil and is the country's most severely threatened biome, requiring a prompt, continuous, and precise mapping and monitoring.

To date, the majority of the studies related to the cerrado's seasonal and land-cover monitoring have been based on optical remote sensing technology. França and Setzer (França and Setzer 1998) as well as Mantovani and Pereira (Mantovani and Pereira 1998) focused on the use of Advanced Very High Resolution Radiometer (AVHRR) and Landsat Thematic Mapper (TM) data to assess the potential of visible and near-infrared multispectral data to discriminate cerrado physiognomies. Ferreira et al. (Ferreira et al. 2003) discriminated three major cerrado units (herbaceous, woody, and forested domains) from simulated Moderate Resolution Imaging Spectroradiometer (MODIS), AVHRR, and Enhanced Thematic Mapper Plus (ETM+) vegetation indices. Ferreira and Huete (Ferreira and Huete 2004) also identified three major land-cover types in the cerrado (agricultural crops; forested areas; and savanna and pastures) by analyzing multitemporal AVHRR vegetation indices.

Although optical remote sensing can be considered a relatively powerful mapping tool, there are some constraints in its usage for vegetation discrimination. For instance, optical data are related only to the top millimeters of the canopy. There-

fore, they present some restrictions to depict structural differences of the cerrado vegetation. Data availability for mono- or multitemporal approaches is dependent on cloud and smoke-free atmospheric conditions.

A good alternative for optical sensors is the microwave spectral region where synthetic aperture radar (SAR) systems operate. SAR sensors can penetrate into clouds and smoke and are independent of solar elevation and azimuth angles. Because of the SAR's canopy penetration capability, significant relations between radar backscatter (σ°, the amount of energy returned to the radar antenna per unit area; Raney 1998) and vegetation parameters such as leaf area index and biomass from empirical and theoretical experiments have been reported in the literature (Ulaby et al. 1984; Paloscia et al. 1999; Inoue et al. 2002). Sano et al. (Sano et al. 2001) obtained encouraging results by analyzing the potential of single-date *Japanese Earth Resources Satellite* (*JERS-1*) SAR data for cerrado's vegetation discrimination. Nevertheless, a major weakness of SAR data for land-cover and land-use mapping and monitoring is the relatively strong soil roughness and soil moisture effects on the backscattered energy from leaves, stalks, and trunks. Moran et al. (Moran et al. 2002) also pointed out the unavailability of commercial, inexpensive ground- or aircraft-based SAR systems to understand the relations between radar images and biophysical properties of land surface. Such systems would be very important to understand the actual effects of roughness and moisture in decreasing the SAR sensitivity to tropical savanna structures.

Because of such complexities and uncertainties of optical and radar sensors, there is a tendency to use the SAR–optical synergism to take advantage of favorable aspects of both sensors simultaneously (Smith et al. 1995; Moran et al. 2002). In this study, we conducted a comparative analysis of the performance and complementarity of the L-band σ° and two vegetation indices, the normalized difference vegetation index (NDVI) and the enhanced vegetation index (EVI), to discriminate the major Brazilian cerrado's physiognomies.

2. Methods

2.1. Study area

The study area corresponded to the Brasilia National Park (BNP), located in the northern Federal District, Brazil, between 15°35′ and 15°45′S latitude and 47°53′ and 48°05′W longitude. The BNP comprises an area of approximately 30 000 ha and is a major savanna research site, with significant ongoing field research from LBA and the Brazilian Environmental Agency (IBAMA). The park also encompasses the major physiognomies encountered in the Brazilian savanna. The vegetation formations in the test site consist of various types of savanna, from grasslands to woodlands plus gallery forests. Sorted by increasing biomass content above the ground, the vegetation units in the park are as follows (Figure 1): cerrado grassland; shrub cerrado; grasslands with termite mounds; wooded cerrado; cerrado woodland; and gallery forest. Table 1 and Figure 2 show some aspects of vegetation structures and conditions encountered in the BNP.

2.2. Analysis approach

Two *JERS-1* SAR images from 22 September 1995 (dry season) and 1 February 1996 (wet season) were acquired from the Japan Aerospace and Exploration

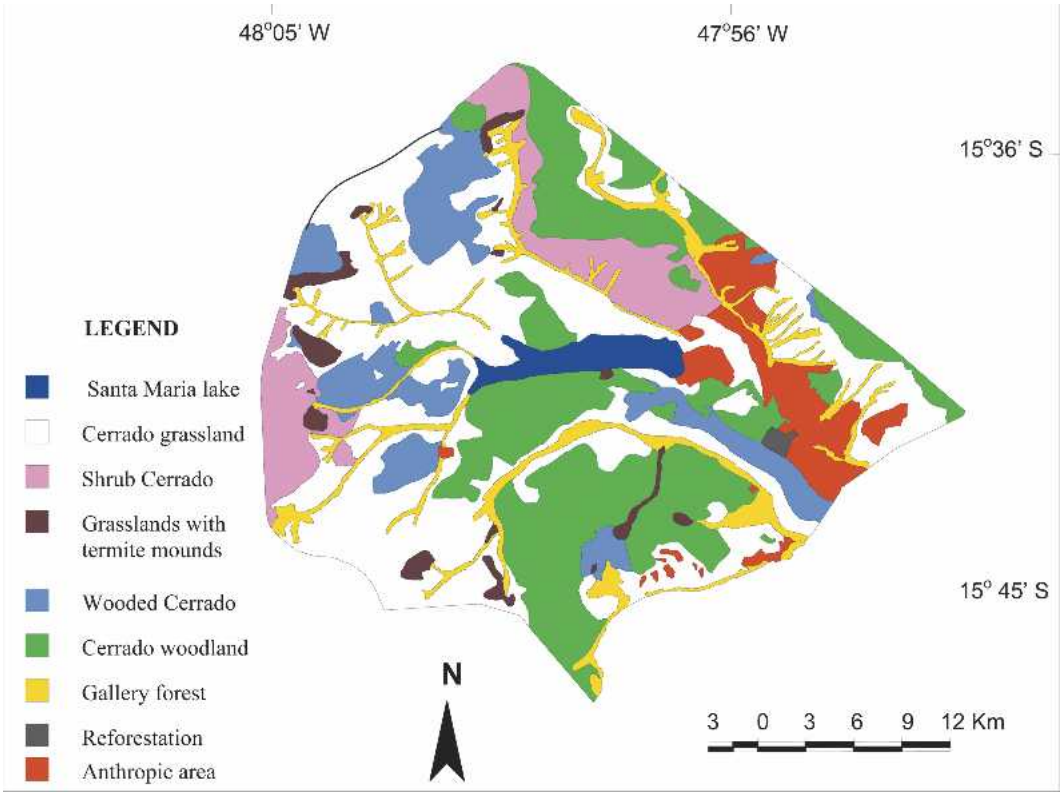

Figure 1. Vegetation map of the Brasilia National Park. (Source: Macedo 1992.)

Agency [JAXA; formerly the National Space Development Agency of Japan (NASDA)]. The *JERS-1* SAR system was operating at a wavelength of 23.5 cm (L band), HH polarization, and a range of incidence angle from 36° (near range) to 41° (far range). The swath width is 75 km, and the nominal spatial resolution, considering three looks in the azimuth direction, is 18 m. The original radar images, with pixel spacing of 12.5 m, were reprocessed to the Universal Transverse of Mercator (UTM) projection and SAD69 reference system.

Several regular polygons (circles) with 25 pixels were used to calculate wet and dry backscattering coefficients over the major cerrado units in the park. The constraint of the sampling size was given by the gallery forest. As its occurrence depends upon the presence of soils with high moisture contents, which are found along streams, its maximum spatial extent away from the streams was not higher than 100 m in the terrain. The values of σ° were calculated using the following equation:

$$\sigma^\circ = 10 \log\left[\left(\frac{\sum_{i=1}^{n} \mathrm{DN}^2{}_i}{n}\right)\right] - 68.5, \quad (1)$$

where DN is digital number and −68.5 dB is the system calibration constant (Shimada 1996).

Table 1. Structural and percent cover characteristics of natural vegetation encountered in the Brasilia National Park. Numbers in italic indicate the predominant average when two layers were identified. (Source: Ferreira et al. 2003.)

Major physiognomies at the Brasilia National Park	Above-ground characteristics	Percent cover of woody layers		Average height of trees (m)		Average tree spacing (m)	Understory percent green cover				Landscape percent green cover			
									Seasonal variation				Seasonal variation	
		Shrubs	Trees	Shrubs	Trees		Wet	Dry	Absolute diff	Relative diff	Wet	Dry	Absolute diff	Relative diff
Cerrado grassland	Open grassland	<1.15	—	<1.4	—	—	43.0	23.1	20.0	46.4	40.0	18.3	21.7	54.2
Shrub cerrado	Open grassland with sparse shrubs	4.3	0.6	0.8/1.6	4.7	33.6	45.2	20.4	24.8	54.9	46.1	25.6	20.5	44.6
Wooded cerrado	Shrubland with sparse trees	24.3	5.4	0.79/1.17	5.3	13.0	42.8	22.0	20.8	48.5	60.4	48.3	12.1	20.1
Cerrado woodland	Mixed grassland, shrubland and mixed trees up to 7 m	20.9	24.5	1.65/2.5	5.7	7.3	37.9	14.5	23.4	61.8	63.4	51.5	11.9	18.8
Gallery forest	Evergreen woodland mainly along streams	—	70–95	—	20–30	—	—	—	—	—	85.5	80.3	5.2	6.0

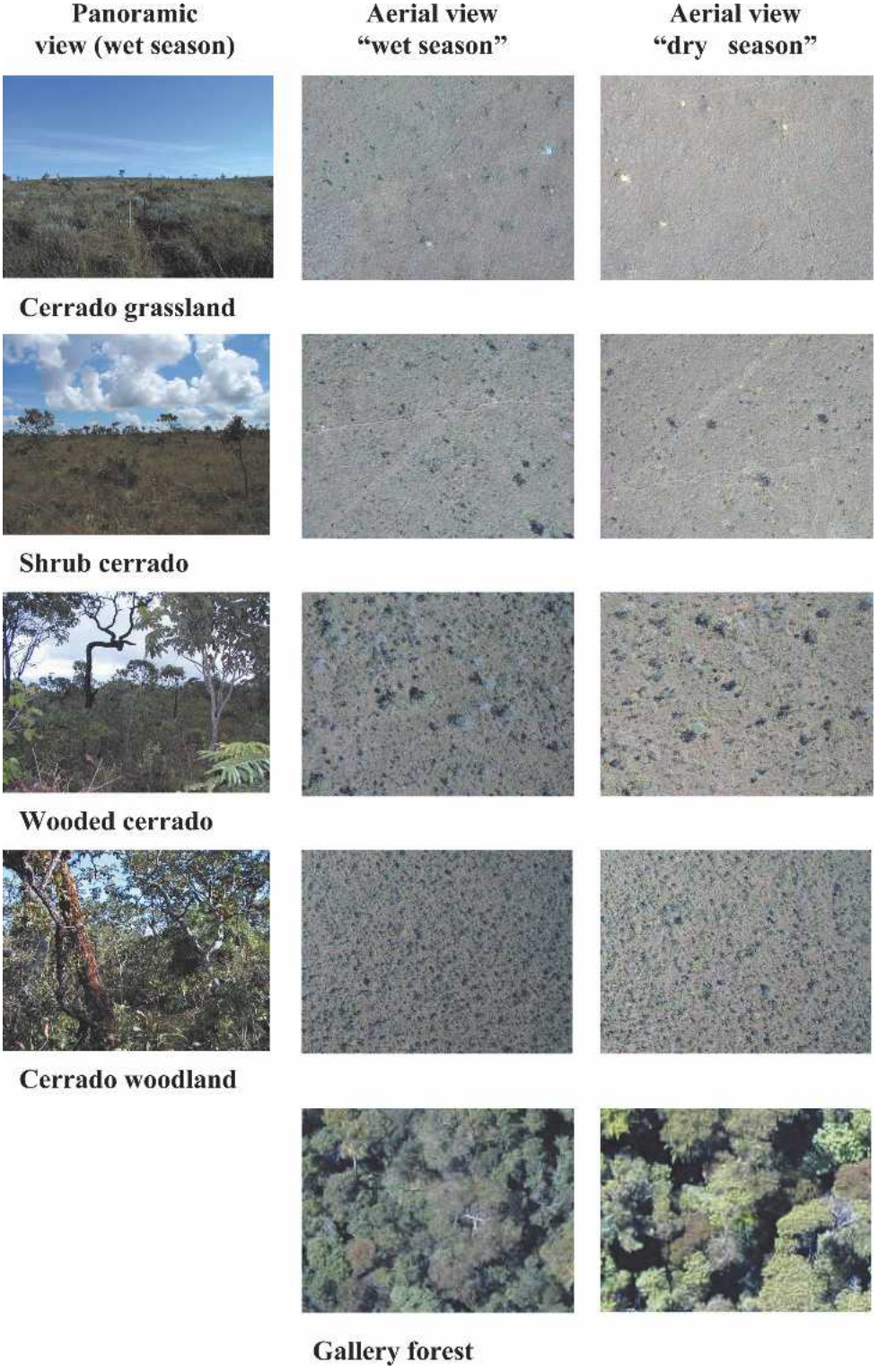

Figure 2. Ground and aerial views of the major cerrado vegetation units found at the Brasilia National Park. (Source: Ferreira et al. 2003.)

The location of the polygons in each cerrado unit was defined by overlaying the vector format, BNP vegetation layer with the dry-season SAR scene. We assumed that, in theory, this was the image that presents the highest correlation with the vegetation structure, which is the major parameter considered by Ribeiro and Walter (Ribeiro and Walter 1998) to define different cerrado units. The same set of polygons were used to calculate the wet season σ°, hereafter named as $\sigma^\circ_{\text{wet}}$ (dry season $\sigma^\circ = \sigma^\circ_{\text{dry}}$).

Two *Landsat-5* TM scenes over the BNP (WRS 221/71) from 24 March 1996 (wet season) and 31 August 1996 (dry season) overpasses were acquired from the Brazilian Institute for Space Research (INPE). For illustration purpose, Figure 3 shows the dry-season *JERS-1* and TM color composite of the study area. The Landsat images were converted to the "top of atmosphere" apparent reflectances and then corrected for Rayleigh scattering and ozone absorption using the 6S radiative transfer code simulations (Vermote et al. 1997).

The corrected reflectance data were spectrally converted to the NDVI (Rouse et al. 1974) and EVI (Huete et al. 1994; Justice et al. 1998) algorithms as follows:

$$\text{NDVI} = \frac{\rho^*_{\text{NIR}} - \rho^*_{\text{Red}}}{\rho^*_{\text{NIR}} + \rho^*_{\text{Red}}}, \tag{2}$$

$$\text{EVI} = 2.5\,\frac{\rho^*_{\text{NIR}} - \rho^*_{\text{Red}}}{(1 + \rho^*_{\text{NIR}} + 6\,\rho^*_{\text{Red}} - 7.5\,\rho^*_{\text{Blue}})}, \tag{3}$$

where ρ^*_{NIR}, ρ^*_{Red}, and ρ^*_{Blue} are the Rayleigh/ozone-corrected reflectances in the NIR, red, and blue bands, respectively.

The same number of polygons used to calculate σ° was also used to derive dry and wet average reflectances. The $\sigma^\circ_{\text{dry}}$, $\sigma^\circ_{\text{wet}}$, and ρ values for all polygons that presented high dispersion were not included in the further analysis. More specifically, all σ° and ρ values higher than one standard deviation of the mean values of each cerrado class were excluded. Potential discrimination among the cerrado physiognomies was evaluated through a linear separability analysis, based on either the Mahalanobis (for multiple datasets) or Euclidian distances (for single datasets) (Schowengerdt 1997), analysis of variance (ANOVA), and Tuckey tests, in which, two vegetation classes were considered to be significantly differentiated (e.g., by either "dry" EVI or "wet" SAR) whenever the null hypothesis (i.e., two classes show identical radiometric responses) was associated with a probability value (p) equal or smaller than 0.05 (Kuehl 1994). All these results were compiled in the form of a discriminant and classification matrices, as well as in a between-groups **F** matrix (**F** statistics), in which the **F** values, proportional to the distance measures, indicate the separability between group means.

3. Results

In this study, we analyzed a total of 935 average backscattering coefficients and vegetation indices from both dry and wet seasons (Table 2). Correlation analysis showed that SAR_{dry} are strongly correlated with SAR_{wet} (Table 3). Such high correlation is probably due to the rainfall nearly null in both radar overpasses,

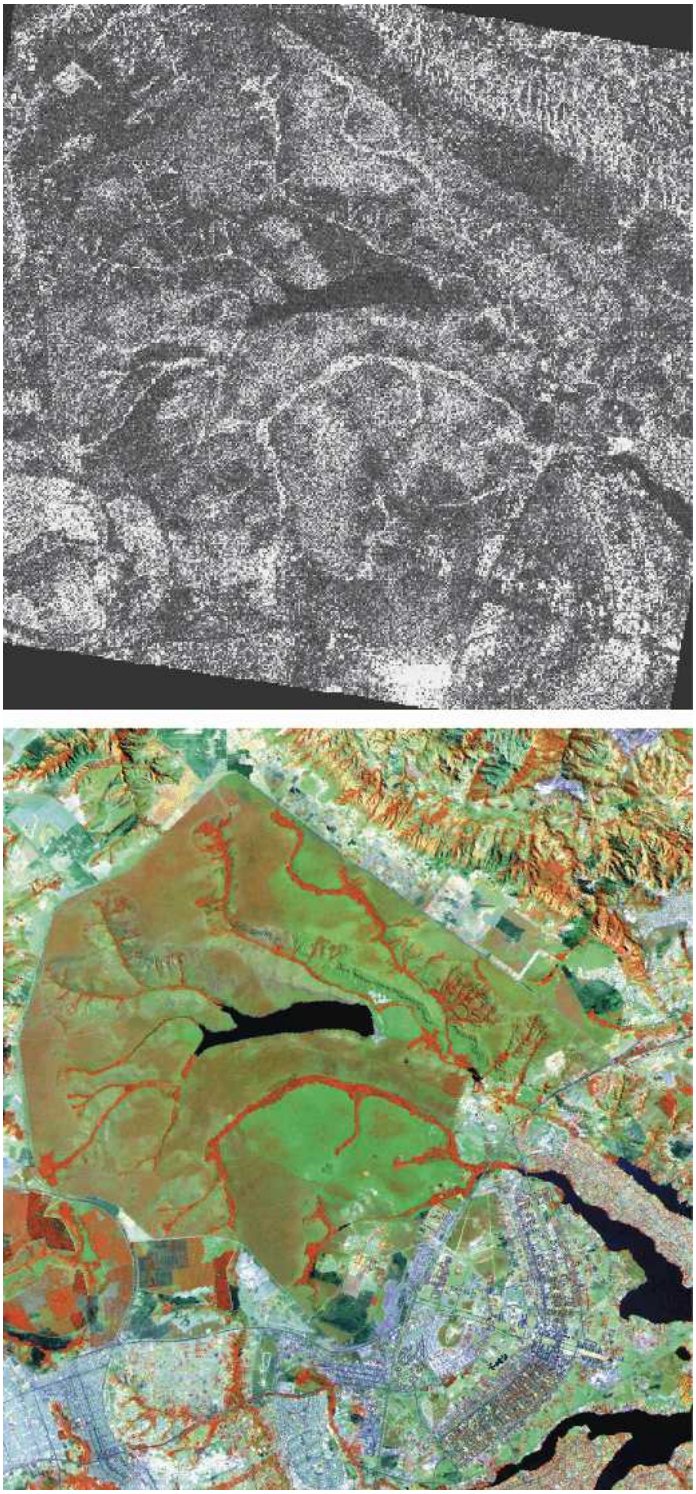

Figure 3. (top) Dry-season images of *JERS-1* SAR and (bottom) color composite of the Landsat/ETM+ over the Brasilia National Park, acquired on 22 Sep 1995 and 31 Aug 1996, respectively.

Table 2. Number of reflectances and backscatter coefficients extracted for each cerrado physiognomy.

Cerrado physiognomy	No. of polygons
Cerrado grassland	338
Shrub cerrado	71
Cerrado grassland or shrub cerrado with termiters	34
Wooded cerrado	137
Cerrado woodland	314
Gallery forest	41
Total	935

leading to relatively low moisture contents of underneath surface soil in both cases. Within the 15-day time period before the two SAR overpassses, there was only one 7-mm rainfall event on 29 January 1995, that is, three days before the wet-season SAR acquisition. Thus, we can assume that the cerrado's vegetation structure and architecture played the major role in both wet and dry SAR scenes analyzed in this study. The two vegetation indices (VIs), when compared within the same season, were also well correlated ($r = 0.98$ and 0.93, respectively). Conversely, SAR and EVI, regardless of seasonality, presented the weakest correlations.

The results of the discriminant analysis suggest that the SAR and VIs provide different types of information and complementarity (Table 4). In contrast to the SAR data, the cerrado grassland was differentiated from shrub cerrado in both NDVI and EVI datasets. On the other hand, wooded cerrado and cerrado woodland could not be distinguished in the $NDVI_{dry}$ dataset. The occurrence of the termite mounds in the herbaceous layer of the park was not distinguished in the $NDVI_{wet}$, EVI_{dry}, and EVI_{wet} datasets. According to the ANOVA (Table 5), the highest average class separabilities were found for SAR_{dry} and SAR_{wet} (2477 and 2344, respectively). Values lower than 515 were recorded for wet-season NDVI and EVI.

The dual season σ° relations (Figure 4) shows that the highest backscattering values are related to the evergreen gallery forests. The L_{HH} transmitting and receiving waves of the *JERS-1* SAR incident in an arboreous canopy cover produce stronger and multiple scattering from trunks and stalks, known as double-bounce scattering (Leckie and Ranson 1998). The lowest values corresponded to the grass-dominated cerrado classes, that is, cerrado grassland, shrub cerrado, and

Table 3. Correlation coefficients between backscattering coefficients and vegetation indices based on datasets from the Brasilia National Park for the wet and dry seasons.

	σ°_{dry}	σ°_{wet}	$NDVI_{dry}$	$NDVI_{wet}$	EVI_{dry}	EVI_{wet}
σ°_{dry}	1.00					
σ°_{wet}	0.98	1.00				
$NDVI_{dry}$	0.72	0.70	1.00			
$NDVI_{wet}$	0.68	0.66	0.85	1.00		
EVI_{dry}	0.62	0.59	0.98	0.84	1.00	
EVI_{wet}	0.51	0.49	0.77	0.93	0.80	1.00

Table 4. Discriminant analysis (based on Tuckey tests) of the dry and wet backscatter and VIs from the Brasilia National Park. Same letters within the columns did not differ significantly at $P < 0.05$.

Cerrado types	Datasets					
	σ°_{dry}	σ°_{wet}	$NDVI_{dry}$	$NDVI_{wet}$	EVI_{dry}	EVI_{wet}
Cerrado grassland	A	A	A	A	A	A
Shrub cerrado	A	A	B	B	B	B
Grassland with the termite mounds	B	B	C	B	B	B
Wooded cerrado	C	C	D	C	C	C
Cerrado woodland	D	D	D	D	D	D
Gallery forest	E	E	E	E	E	E

Table 5. ANOVA of the dry and wet backscatter and VIs from the Brasilia National Park.

Statistical parameters	Datasets					
	σ°_{dry}	σ°_{wet}	$NDVI_{dry}$	$NDVI_{wet}$	EVI_{dry}	EVI_{wet}
F	2447	2344	1177	514	1232	313
Adjusted r^2	0.93	0.93	0.86	0.73	0.87	0.63
P	<0.05	<0.05	<0.05	<0.05	<0.05	<0.05

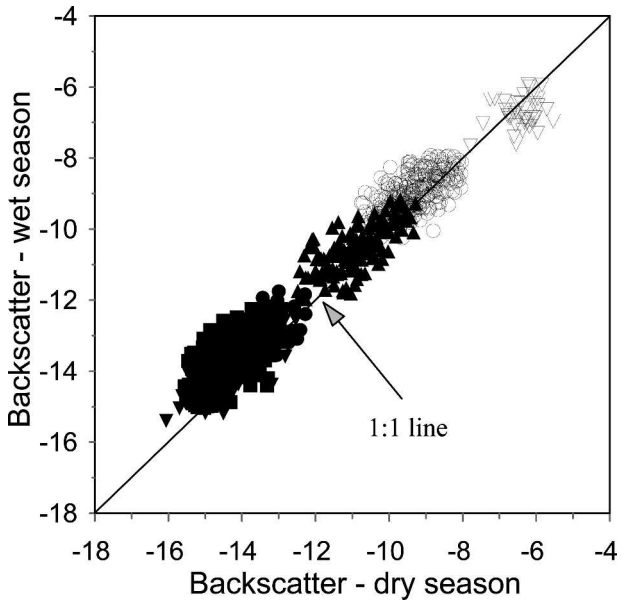

Figure 4. Comparison between dry- and wet-season backscatter of the Brasilia National Park land covers (+ = cerrado grassland; ▼ = shrub cerrado; ● = cerrado grassland/shrub cerrado with termite mounds; ▲ = wooded cerrado; ◯ = cerrado woodland; and ∇ = gallery forest).

grassland with termite mounds. The majority of the σ° values located close to the 1:1 line and the similar range of σ°_{wet} (−15.39 to –5.93 dB) in relation to the σ°_{dry} (−16.06 dB to –5.53 dB) confirm the previous finding about the seasonality independence of the SAR data over the BNP. However, slightly higher backscattering coefficients in the σ°_{wet} can be noticed for the herbaceous layers or even for the mixed grassland/shrubland/woodland covers (wooded cerrado and cerrado woodlands), but not for the gallery forests. Indeed, grasslands are more responsive to variations in rainfall or, ultimately, to variations in soil moisture conditions because of their relatively lower biomass density. The figure also exhibits the possibility of identification of four groups of cerrado classes in the SAR images: (a) savanna grassland, shrub savanna, and grasslands with termite mounds; (b) wooded savanna; (c) savanna woodland; and (d) gallery forest. In other words, active microwave remote sensing data can easily separate the grasslands, mixed grassland/shrubland/woodlands, and woodlands of tropical savannas.

The visual inspection of the $NDVI_{dry}$ versus $NDVI_{wet}$ and especially for the EVI_{dry} versus EVI_{wet} crossplots shows significant seasonal variations in the semideciduous vegetation activities from the BNP (Figure 5). This indicates high photosynthetic activity and high green biomass accumulation in the study area during the wet season (March) and a significant soil water deficit and low levels of green biomass in the dry season (September). EVI values were generally lower than NDVI values. The dynamic ranges of EVI values varied from 0.05 to 0.30 (dry season) and from 0.25 to 0.55 (wet season), a much smaller range than that of the NDVI [0.15 to 0.65 (dry season) and 0.35 to 0.70 (wet season)]. Specifically, for gallery forest, we found low NDVI variation (from 0.57 to 0.67 on average, for dry and wet seasons, respectively), but a surprisingly great variation in the EVI (from 0.25 to 0.50 on average, for dry and wet seasons, respectively). Figure 4 illustrates the capability of the monotemporal VIs to distinguish two main vegetation domains: grassland plus mixed grassland/shrubland/woodland and woodland (gallery forest).

The statistical analysis based on discriminant analysis and ANOVA demonstrated the potential of SAR–VI synergism to discriminate different types of cerrado units. Although the **F** values showed in Table 4 indicate better results for the SAR data (**F** = 2447 and 2344 for dry and wet signals, respectively), we can notice spectral confusion between cerrado grassland and shrub cerrado, which does not happen with the VI values, regardless of lowest **F** values.

Table 6 shows the performance of the total correct classification (CC) of several individual and combined datasets. EVI and NDVI, regardless of seasonality, showed the lowest performances (CC < 63%; CC = % correct classification). However, when the two VIs from the two seasons are all combined, the discrimination accuracy increased significantly (CC = 79%). Overall, individual radar backscattering coefficients showed better performance than that from the VIs. As expected, σ°_{wet}, σ°_{dry}, and $\sigma^\circ_{(wet\ \&\ dry)}$ showed similar results (CC = 69, 69, and 70, respectively). This is consistent with vegetation structure being the driving factor in radar backscatter from the park. The combination of SAR and VI data from a single season [$(\sigma^\circ$ and $EVI)_{dry}$, $(\sigma^\circ$ and $NDVI)_{dry}$, $(\sigma^\circ$ and $EVI)_{wet}$, and $(\sigma^\circ$ and $NDVI)_{wet}$] showed moderate improvement (72% < CC < 74%). The best performance was obtained when all data (σ° and VI, dry and wet seasons) are grouped together: CC = 85%.

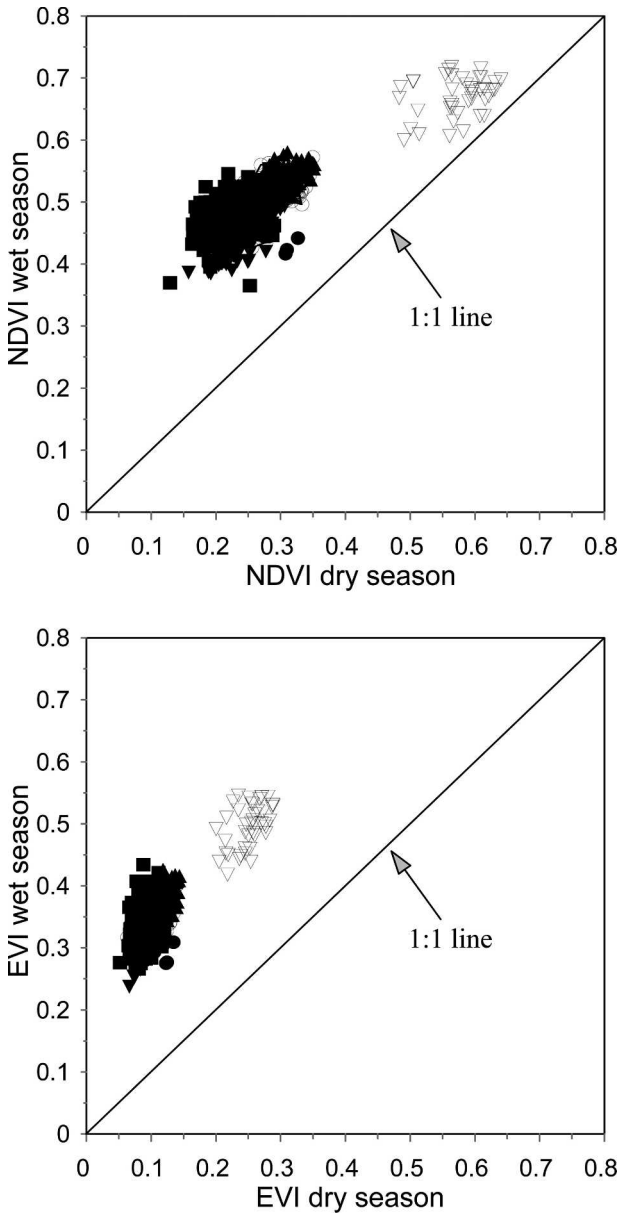

Figure 5. Comparison of dry- and wet-season (a) NDVI and (b) EVI for the Brasilia National Park land covers (legend as in Figure 3).

4. Conclusions

A comparative analysis of *JERS-1* SAR and optical NDVI and EVI data from dry and wet seasons from the Brasilia National Park was conducted to assess their individual and combined potential to map cerrado physiognomies and to monitor cerrado seasonal dynamics. The results indicated that vegetation structure plays the major role in the backscattering processes over the Brazilian tropical savanna.

Table 6. Percentage of correct classification for different combinations of SAR and VI datasets from the Brasilia National Park.

Dataset	Percent correct classification
EVI_{wet}	35
EVI_{dry}	51
$NDVI_{wet}$	52
$NDVI_{dry}$	52
$EVI_{(dry\ \&\ wet)}$	53
$NDVI_{(dry\ \&\ wet)}$	63
σ°_{wet}	69
σ°_{dry}	69
$\sigma^{\circ}_{(dry\ \&\ wet)}$	70
$(\sigma^{\circ}$ and $EVI)_{dry}$	72
$(\sigma^{\circ}$ and $NDVI)_{dry}$	72
$(\sigma^{\circ}$ and $EVI)_{wet}$	74
$(\sigma^{\circ}$ and $NDVI)_{wet}$	74
$(EVI$ and $NDVI)_{(dry\ \&\ wet)}$	79
$(\sigma^{\circ}$ and $VI)_{(dry\ \&\ wet)}$	84

Considering both techniques alone, the performance of the L_{HH} surpassed the two Landsat VIs in terms of mapping the cerrado physiognomies. However, a combination of dual temporal radar backscatter with NDVI and EVI at a time indicated a higher capability to identify cerrado vegetation types. The sensitivity of the VIs to the seasonal vegetation variations demonstrated their potential to monitor and assess the temporal variations of the cerrado conditions.

Acknowledgments. The Brazilian National Research Council (CNPq) is providing individual research grants for the first two authors. The National Space Development Agency (NASDA) of Japan provided the SAR images as part of the *JERS-1* Verification Program (Proposal J-1801). This work was partially supported by the MODIS Contract NAS5-31364 (Alfredo R. Huete).

References

Eiten, G., 1993: Cerrado's vegetation (in Portuguese). *Cerrado: Caracterizacao, Ocupacao e Perspectivas*, 2d ed, M. N. Pinto, Ed., Universidade de Brasilia, 17–73.

Ferreira, L. G., and A. R. Huete, 2004: Assessing the seasonal dynamics of the Brazilian Cerrado vegetation through the use of spectral vegetation indices. *Int. J. Remote Sens.,* **25,** 1837–1860.

——, H. Yoshioka, A. R. Huete, and E. E. Sano, 2003: Seasonal landscape and spectral vegetation index dynamics in the Brazilian Cerrado: An analysis within the Large Scale Biosphere–Atmosphere Experiment in Amazonia (LBA). *Remote Sens. Environ.,* **87,** 534–550.

França, H., and A. W. Setzer, 1998: AVHRR temporal analysis of a savanna site in Brazil. *Int. J. Remote Sens.,* **16,** 3127–3140.

Huete, A. R., C. Justice, and H. Liu, 1994: Development of vegetation and soil indices for MODIS-EOS. *Remote Sens. Environ.,* **49,** 224–234.

——, K. Didan, T. Miura, E. P. Rodriguez, X. Gao, and L. G. Ferreira, 2002: Overview of the

radiometric and biophysical performance of the MODIS vegetation indices. *Remote Sens. Environ.,* **83,** 195–213.

Inoue, Y., T. Kurosu, H. Maeno, S. Uratsuka, T. Kozu, K. Dabrowska-Zielinska, and J. Qi, 2002: Season-long daily measurements of multifrequency (Ka, Ku, X, C and L) and full-polarization backscatter signatures over paddy rice field and their relationship with biological variables. *Remote Sens. Environ.,* **81,** 194–204.

Justice, C. O., and Coauthors, 1998: The Moderate Resolution Imaging Spectroradiometer (MODIS): Land remote sensing for global change research. *IEEE Trans. Geosci. Remote Sens.,* **36,** 1–22.

Kuehl, R. O., 1994: *Statistical Principles of Research Design and Analysis.* 1st ed. Duxbury Press, 681 pp.

Leckie, D. G., and K. J. Ranson, 1998: Forestry applications using imaging radar. *Principles and Applications of Imaging Radar*, Vol. 2, 3d ed., *Manual of Remote Sensing,* F. M. Henderson and A. J. Lewis, Eds., John Wiley & Sons, 435–509.

Macedo, J., 1992: Soil studies from the Brasilia National Park (in Portuguese). Appendix 2, Technical Report for subsidizing the review of the Brasilia National Park monitoring plan, 39 pp.

Mantovani, J. E., and A. Pereira, 1998: Estimating the integrity of the cerrado vegetation cover through the Landsat-TM data (in Portuguese). *Proc. Brazilian Symp. on Remote Sensing,* Santos, Sao Paulo, Brazil, Brazilian Institute for Space Research, CD-ROM.

Moran, M. S., D. C. Hymer, J. Qi, and Y. Kerr, 2002: Comparison of ERS-2 SAR and Landsat TM imagery for monitoring agricultural crop and soil conditions. *Remote Sens. Environ.,* **79,** 243–252.

Paloscia, S., G. Macelloni, P. Pampaloni, and S. Sigismondi, 1999: The potential of C- and L-band SAR in estimating vegetation biomass: The ERS-1 and JERS-1 experiments. *IEEE Trans. Geosci. Remote Sens.,* **37,** 2107–2110.

Raney, R. K., 1998: Radar fundamentals: Technical perspective. *Principles and Applications of Imaging Radar*, Vol. 2, 3d ed., *Manual of Remote Sensing,* F. M. Henderson and A. J. Lewis, Eds., John Wiley & Sons, 9–130.

Ribeiro, J. F., and T. M. B. Walter, 1998: The major physiognomies in the Brazilian Cerrado region (in Portuguese). *Cerrado: Ambiente e Flora*, S. M. Sano and S. P. Almeida, Eds., Embrapa-CPAC, 169–188.

Roberts, D. A., M. Keller, and J. V. Soares, 2003: Studies of land-cover, land-use and biophysical properties of vegetation in the Large Scale Biosphere Atmosphere experiment in Amazônia. *Remote Sens. Environ.,* **87,** 377–388.

Rouse, J. W., R. H. Haas, J. A. Schell, and D. W. Deering, 1974: Monitoring vegetation systems in the Great Plains with ERTS. *Proc. Third Earth Resources Technology Satellite Symp.,* Vol. 1, Greenbelt, MD, NASA GSFC, SP-351, 309–317.

Sano, E. E., G. C. C. Pinheiro, and P. R. Meneses, 2001: Assessing JERS-1 synthetic aperture radar data for vegetation mapping in the Brazilian savanna. *J. Remote Sens. Soc. Japan,* **21,** 158–167.

Schowengerdt, R. A., 1997: *Remote Sensing: Models and Methods for Image Processing*. 2d ed. Academic Press, 522 pp.

Shimada, M., 1996: Radiometric and geometric calibration of JERS-1 SAR. *Adv. Space Res.,* **17,** 79–88.

Smith, A. M., D. J. Major, R. L. McNeil, W. D. Willms, B. Brisco, and R. J. Brown, 1995: Complementarity of radar and visible-infrared sensors in assessing rangeland conditions. *Remote Sens. Environ.,* **52,** 173–180.

Ulaby, F. T., C. T. Allen, G. Eger III, and E. Kanemasu, 1984: Relating the microwave backscattering coefficient to leaf area index. *Remote Sens. Environ.,* **14,** 113–133.

Vermote, E. F., D. Tanre, J. L. Deuze, M. Herman, and J. J. Morcrette, 1997: Second simulation of the satellite signal in the solar spectrum, 6S: An overview. *IEEE Trans. Geosci. Remote Sens.,* **35,** 675–686.